GSI Annual Report 2002 (extracts)

Chemistry

Nuclear Structure

First results of the CALLISTO-experiment: Evidence for the formation of a hassate(VIII)

A. von Zweidorf[1], R. Angert[1], W. Brüchle[1], S. Bürger[2], K. Eberhardt[2], R. Eichler[1,3], H. Hummrich[2], E. Jäger[1], R. Jera[2], H.-O. Kling[2], J. V. Kratz[2], U. Krille[2], B. Kuczewski[2], G. Langrock[2], G. Lehr[2], M. Mendel[2], A. Nähler[2], A. Peil[2], V. Pershina[1], U. Rieth[2], M. Schädel[1], B. Schausten[1], E. Schimpf[1], H.-J. Schött[1], E. Stiel[1], P. Thörle[2], N. Trautmann[2], K. Tsukada[4], N. Wiehl[2], G. Wirth[1]

[1]Gesellschaft für Schwerionenforschung, Darmstadt, [2]Institut für Kernchemie, Johannes Gutenberg-Universität Mainz, [3]now at PSI, Villigen, [4]JAERI, Tokai

In October/November 2002, after an intensive optimization of many experimental parameters, the CALLISTO-project finally led to a hassium chemistry experiment [1] at the UNILAC. Since it has been predicted, that hassium forms a volatile tetroxide [2], which was recently confirmed by C. Düllmann et al. [3], we decided to investigate this compound of hassium.

For the very volatile OsO_4, it is known that it dissolves in strongly basic alkali hydroxide solutions thereby forming red, diamagnetic osmates(VIII) of stoichiometry $[OsO_4(OH)_2]^{2-}$. In previous beamtimes, in which OsO_4 was produced in-situ directly behind the target [4], we demonstrated, that the volatile OsO_4 deposits effectively on NaOH surfaces from humid He gas.

This behaviour was used to design a continuously working system for the formation, transport, deposition and detection of OsO_4 and HsO_4 [1]. This system, which uses 4 computer-controlled valves and 4 detection arrays, each with 4 alpha-detectors [5], combines the advantages of a continuously operating system and adds the possibility to change the deposition material, a thin layer of NaOH on a plate of stainless steel, on a regular basis without interrupting the experiment. Changing the deposition material is necessary, as the deposition efficiency decreases with time [1].

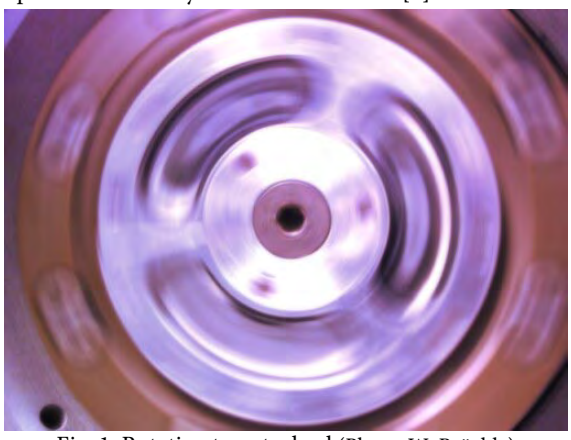

Fig. 1: Rotating target wheel (Photo: W. Brüchle)

A rotating target wheel (Fig. 1), containing two ^{248}Cm-targets of 0.6 mg/cm^2 each and one ^{152}Gd-enriched-Gd-target, was irradiated with $1.18 \cdot 10^{18}$ ^{26}Mg beam particles at 144-149 MeV. In the second part of the beamtime, the ^{152}Gd-target segment was replaced with a ^{248}Cm/^{152}Gd-hybrid target to enhance the hassium production. This target wheel was irradiated with a total amount of $1.64 \cdot 10^{18}$ particles at 142-150 MeV.

Os and Hs recoils, synthesized simultaneously, are stopped in a mixture of He and O_2 inside a recoil chamber especially designed for this purpose. This results in an in-situ formation of volatile oxides, which are carried out with the He-gas jet.

In our experiment, about 290 deposition plates were coated with NaOH and successfully used. The main part of the OsO_4 deposits in the first detection array. The distribution of the activity of OsO_4 in the detection system is shown in Fig. 2.

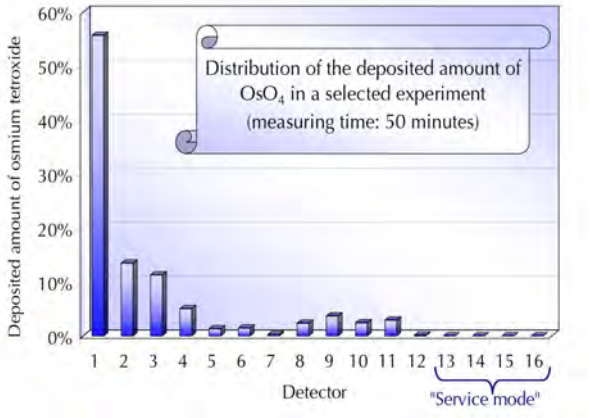

Fig. 2: Distribution of Os in the detection system

The data evaluation is in progress. A first and preliminary analysis shows α-α-decay chains and α-SF correlations which we tentatively attribute to the decay of Hs isotopes. For the first time, a chemical reaction has been performed with hassium tetroxide. Since the observed deposition of HsO_4 under the conditions of this CALLISTO set-up is only possible, if this volatile substance reacts with NaOH, we conclude, that HsO_4 reacted with NaOH. Since very similar properties for OsO_4 and HsO_4 can be expected [2], we suppose, that sodium dihydroxo-tetraoxohassate(VIII) was formed:

$$2NaOH + HsO_4 \rightarrow Na_2[HsO_4(OH)_2]$$

So, if the off-line analysis substantiates the above findings, for the first time in the history of element 108, a classical acid-base-reaction was successfully carried out one-atom-at-a-time using its tetroxide.

Besides it should be noted, that ^{34m}Cl has been produced as a byproduct in the target chamber. It was deposited on the alkaline surface too and was identified via γ-spectroscopy. Generally, the CALLISTO set-up may be able to investigate the chemistry of other volatile substances, which are able to react with reactive surfaces, too.

References

[1] A. von Zweidorf *et al.*, this GSI Scientific Report
[2] V. Pershina *et al.*, J. Chem. Phys. **115** (2001), p. 792
[3] C. Düllmann *et al.*, Nature, 418, (2002) 859
[4] A. von Zweidorf *et al.*, GSI Scientific Report 2001, p. 181
[5] Pictures are available at *http://www.callisto.ws*

CALLISTO - an improved setup for the chemical investigation of hassium tetroxide

A. von Zweidorf[1], R. Angert[1], W. Brüchle[1], S. Bürger[2], K. Eberhardt[2], R. Eichler[1,3], H. Hummrich[2], E. Jäger[1], R. Jera[2], H.-O. Kling[2], J. V. Kratz[2], U. Krille[2], B. Kuczewski[2], G. Langrock[2], G. Lehr[2], M. Mendel[2], A. Nähler[2], A. Peil[2], V. Pershina[1], U. Rieth[2], M. Schädel[1], B. Schausten[1], E. Schimpf[1], H.-J. Schött[1], E. Stiel[1], P. Thörle[2], K. Tsukada[4], N. Wiehl[2], G. Wirth[1]

[1]Gesellschaft für Schwerionenforschung, Darmstadt, [2]Institut für Kernchemie, Johannes Gutenberg-Universität Mainz, [3]now at PSI, Villigen, [4]JAERI, Tokai

It has been predicted [1] and confirmed [2], that hassium forms a volatile tetroxide. The first attempt to study a chemical reaction of this compound, and to learn more about the chemical behaviour of Hs, is described in a companion contribution [3].

For this purpose, CALLISTO [4] has been developed in recent years. This system, which is in principle gas chemistry using reactive surfaces, was completely redesigned to integrate all the results of the many preliminary experiments.

The volatile tetroxide is formed in-situ in the target chamber, where the recoils are stopped in the jet gas (a mixture of 1 l/min He and 0.1 l/min O_2)[5]. At the exit of the target chamber, the gas flow passes a quartz glass tube containing a quartz wool plug, both heated to 500 °C in order to complete the oxidation of osmium and hassium to the tetroxide. The gas is transported via a 13 m long PTFE capillary to the detection system.

Because water seems to influence the deposition of OsO_4 on the NaOH surface [6], it was necessary to introduce it into the chemical system. As H_2O cannot be added before the He passes the target chamber (it prohibits an accurate beam current measurement), it was added after the target chamber and before the detection system.

For that reason, a special moisturizing unit was designed for CALLISTO. It consists of a large, thermostated moisturizer [7], which continuously adds at a defined temperature (30 °C) water to a second helium jet (0.1 l/min with the option to use 0.05 - 2 l/min). This humidified helium passes through a declusterizer at 200 °C to evaporate all remaining water aerosols. Thereafter, the humidity of the gas was monitored with a dew-point transmitter (~20 g H_2O per kg gas). This moisturized helium is added to the jet gas from the target chamber, containing only a few ppm of water and resulting in a humidity of about 2 g H_2O per kg gas in the final gas jet. This jet is then distributed through a system of 4 computer-controlled valves to 4 detection arrays (Fig. 1).

During an experiment, the He gas is flowing through 3 detection arrays, whereas 1 detection array is cut off from the gas flow; it is in a "service mode" to change the deposition material. We used a thin layer of NaOH as a deposition material, which was prepared by coating plates of stainless steel with 1M ethanolic NaOH and by drying these plates. Every 60 minutes, the valves were automatically switched and the deposition plate of the detection array, being in the "service mode", was manually changed, cleaned and recoated. Thus, a continuously working detection and deposition system was realized.

The surface of the deposition material looses reactivity with time [6]. One possible explanation is, that NaOH is partially neutralized by CO_2, which is an impurity of the used gases and

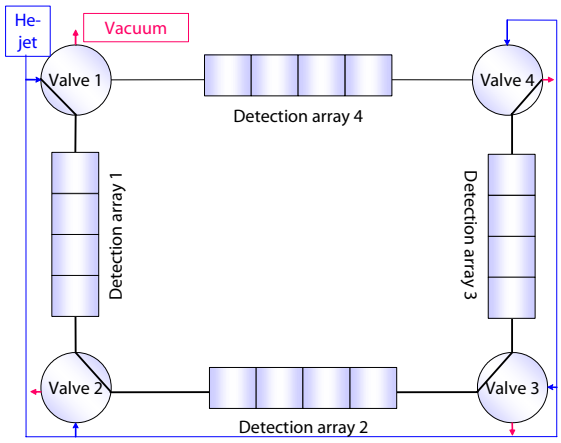

Fig. 1: Schematic of CALLISTO's valve- and detection system

probably formed by a reaction of the carbon beam dump with the oxygen of the jet gas, too. The Na_2CO_3 has a decreased reactivity and shows only a yield of about 50%, compared to NaOH.

After the volatile oxides (OsO_4, HsO_4) are deposited, their α-decay and spontaneous fission can be detected with the detection arrays, each consisting of four (10x10) mm^2 large PIN-diodes facing the deposition material (Fig. 2).

Fig. 2: Detection array (Photo: A. Zschau / G.Otto, GSI)

The CALLISTO set-up has been successfully used to produce and deposit OsO_4 and HsO_4 during the beamtime October/November 2002 [3]. The analysis of the data is still in progress and more information will be available soon.

References

[1] V. Pershina *et al.*, J. Chem. Phys. **115** (2001), p. 792
[2] C. Düllmann *et al.*, Nature, 418, (2002) 859
[3] A. von Zweidorf *et al.*, this GSI Scientific Report
[4] A. von Zweidorf *et al.*, GSI Scientific Report 2001, p. 181
[5] A. von Zweidorf *et al.*, GSI Scientific Report 1999, p. 236
[6] A. von Zweidorf *et al.*, this GSI Scientific Report
[7] Pictures are available at *http://www.callisto.ws*

Influence of water on the deposition of osmium tetroxide on alkaline surfaces

A. von Zweidorf[1], R. Angert[1], W. Brüchle[1], R. Eichler[1,3], E. Jäger[1], J. V. Kratz[2], G. Langrock[2], M. Mendel[2], M. Schädel[1], B. Schausten[1], E. Schimpf[1], P. Thörle[2] , G. Wirth[1]

[1]Gesellschaft für Schwerionenforschung, Darmstadt, [2]Institut für Kernchemie, Johannes Gutenberg-Universität Mainz, [3]now at PSI, Villigen

It is known, that the very volatile osmium tetroxide can be deposited directly on alkaline surfaces [1]:

$$2OH^- + OsO_4 \rightarrow [OsO_4(OH)_2]^{2-}$$

This behaviour has been studied to test its application to investigate the chemical properties of hassium tetroxide, which should have similar properties as OsO_4 [2].

In our experiment, Os was produced in-situ using the CALLISTO-setup [3] and irradiating a rotating wheel of barium targets with a beam of ^{40}Ca. OsO_4, formed in the recoil chamber with O_2 in the He gas, was deposited on stainless steel plates, coated with 1 M and, in another experiment, with 2.8 M ethanolic NaOH solution. The deposited amount of OsO_4 decreased with the time of the experiment significantly (Fig. 1).

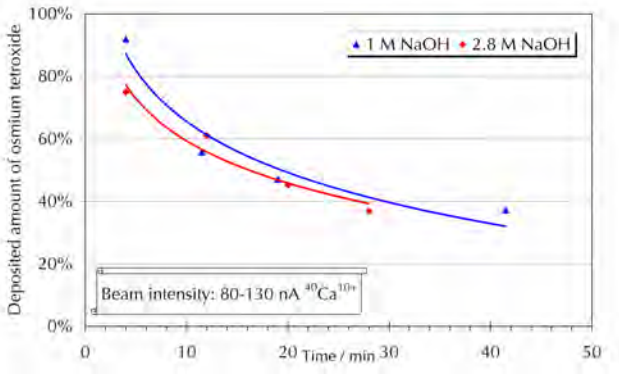

Fig. 1: Deposition of OsO_4 using unmoisturized gases

Because macroscopic amounts of NaOH cannot be fully neutralized by microscopic amounts of OsO_4, and the same behaviour has been observed for both coatings, other effects seem to influence the reaction of OsO_4 with NaOH.

Because this reaction is a classic acid-base-reaction, water may influence this process greatly. The used gases (He, O_2) always contain water as an impurity (typically 5 ppm for He 4.6), so it was supposed, that the deposition process may benefit from an increased amount of water in this chemical system.

To increase the humidity of this system, a special moisturizer was designed [4]. It consists of a thermostated reservoir of water with an adequate quantity for a hassium experiment. It is passed by a flow of 0.05 - 2 l/min helium, which passes thereafter a declusterizer (a glass frit at 200 °C), because water particles may be formed in the moisturizing process. The humidity of the gas was examined with a dewpoint transmitter. The moisturized helium was added after the jet leaves the target chamber (Fig. 2).

To test this method, a rotating wheel with Ce-targets was irradiated with an ^{40}Ar-beam. The formed OsO_4 was deposited using plates coated with 1 M ethanolic NaOH. A mixture of 0.9 l/min He and 0.1 l/min O_2 passed the target chamber and was mixed with 0.05 l/min moisturized He. Keeping the temperature of the moisturizer at 30 °C resulted in a humidity of about 20 g H_2O per kg gas in the moisturized He, leading to

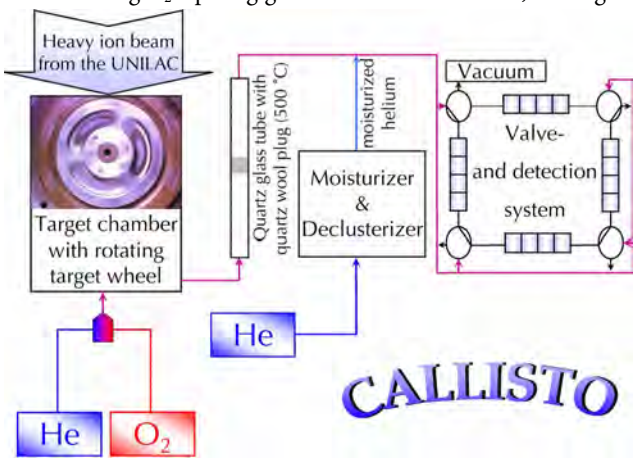

Fig. 2: Scheme of the CALLISTO-setup

about 1 g H_2O per kg gas in the final gas mixture.

Under these conditions is it possible to deposit about 80% of the OsO_4 on the alkaline surface (Fig. 3).

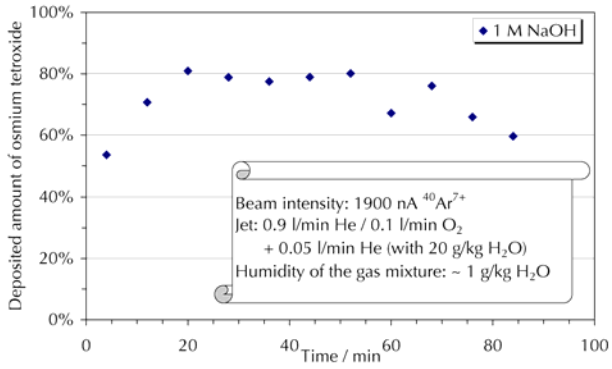

Fig. 3: Deposition of OsO_4 using moisturized gases

This leads to the conclusion, that water is necessary for a fast and nearly quantitative deposition of OsO_4 on sodium hydroxide. The observed decrease after 60 min could be explained with the fact, that disturbing CO_2, which is an impurity of the used gases (1 ppm for He 4.6) and may be formed via a reaction of the graphite beam dump with the jet gases, could react with the alkaline surface, forming the much less absorbing Na_2CO_3.

References

[1] A. von Zweidorf *et al.*, GSI Scientific Report 2001, p. 181
[2] V. Pershina *et al.*, J. Chem. Phys. **115** (2001), 792
[3] A. von Zweidorf *et al.*, this GSI Scientific Report
[4] Pictures are available at *http://www.callisto.ws*

Model Experiments for the chemical investigation of element 112

S. Soverna [1,2], R. Eichler [1,2], H.W. Gäggeler [1,2], F. Haenssler [1,2], Z. Qin [1,2],
R. Dressler [2], B. Eichler [2] and D. Piguet [2]

[1]University of Bern, Switzerland, [2]Paul Scherrer Institut, Switzerland

The systematic order of the periodic table suggests that element 112 (E112) belongs to group 12, hence its electronic ground state configuration is assumed to be Rn:$6d^{10}7s^2$. Direct relativistic effects may result in a stronger binding of the electrons in the spherical relativistic s and $p_{1/2}$ orbitals. Due to this strong relativistic shell stabilization of the 7s orbital Pitzer [1] suggested in 1973 that E112 could behave as chemically inert as a noble gas. However, indirect relativistic effects imply a destabilization of the 6d electron orbitals, leading to a possible transition metal behaviour of element 112. In 1976 Eichler [2] predicted a noble metallic behaviour of E112, more similar to Hg. Therefore, the primary scientific goal of the chemical investigation of E112 must be the differentiation between a noble metallic character and a noble-gas like behaviour. The amount of the adsorption enthalpy of E112 on a metallic surface is decisive on whether a van der Waals interaction or a metallic bond with the surface is observed. Hence, an advanced version of the chemical separator IVO [3] suitable for the chemical investigation of the element 112 was developed. The set-up was tested on-line with short-lived Hg-isotopes, produced in nuclear fusion reactions of ^{20}Ne and Yb (enriched in ^{168}Yb) at the PHILIPS cyclotron at Paul Scherrer Institute, and with ^{219}Rn emanating from an ^{227}Ac source. The inner surface of the newly designed recoil chamber of IVO is completely covered by a quartz insert to inhibit an adsorption of a potentially metallic E112 on metal surfaces.

Dried 1 l/min He carrier gas flushes an ^{227}Ac source before entering the recoil chamber. Products of the heavy ion induced nuclear fusion reaction recoiling backwards out of the target are thermalized in this gas. Only gaseous products are swept out of the recoil chamber through an open quartz column. Subsequently, they were transported to a nearby oven with a quartz wool filter heated up to 850°C through a connected PFA-capillary. Aerosol particles produced in beam induced sputtering processes in the target material and in the beam dump are stopped in this filter. The volatile products pass this filter and a connected 10 m long PFA-capillary to a Ta-Ti-getter heated up to 1000 °C. Trace amounts of water are removed from the carrier gas by this getter. Subsequently, the remaining gaseous products enter the COLD thermochromatography. The new version of this device consists of 32 silicon PIN-photodiodes with 10 x 9.8 mm^2 active area mounted in a row at a distance of 1.6 mm opposite to an Au surface and forming a rectangular gas chromatographic column. Thus, a spectroscopy of α- or SF-decay from atoms adsorbed on the Au surface is provided in 2-π detection geometry. A temperature gradient from 6 °C to –183 °C is applied to the detector array (see Fig.1, dashed lines). The whole detector set-up is placed into a steel box, which is evacuated to 1 mbar in order to isolate it thermally and to eliminate the moisture from the surrounding air. Similar to mercury the formation of a metal bond with a metallic Au surface is expected for element 112 [4]. Therefore, gold was selected as chromatographic surface. Furthermore, its chemical inertness to oxidation provides a clean metallic chromatographic surface. An over-all transport efficiency of 80 % was determined for $^{186-190}$Hg at a transport time of less than 25 s. Separation factors of about 10^6 have been determined for lanthanides (model elements for the heavy actinides) in experiments with ^{156}Yb, produced in the reaction ^{142}Nd(^{20}Ne, 6n). The deposition distributions of Hg and Rn in the detector array (grey and black bars, respectively) are shown together with results from Monte Carlo simulations (dashed and white bars, respectively) in Fig.1.

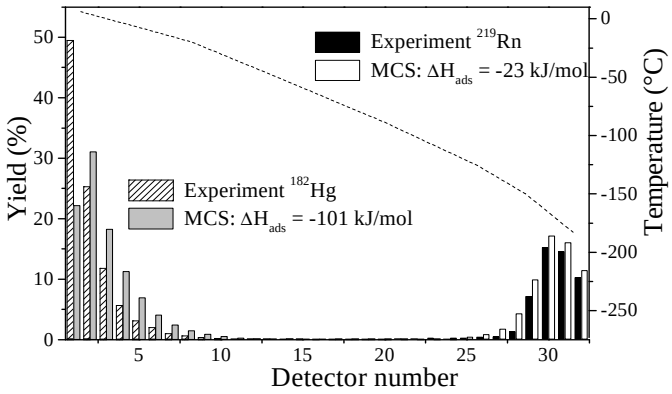

Fig. 1: Thermochromatograms of ^{182}Hg and ^{219}Rn on Au at a carrier gas flow of 1 l/min .

The spontaneous, diffusion controlled deposition of Hg (ΔH_{ads}= -101 kJ/mol [5]) on Au is well reproduced by a Monte Carlo simulation of gas chromatography. For Rn the deposition pattern is reproduced best assuming an adsorption enthalpy of ΔH_{ads} = -23 kJ/mol. In earlier thermochromatographic experiments with Rn in ice columns an adsorption enthalpy of -20 kJ/mol was determined [6]. The low adsorption interaction in the recent experiment indicates ice formation at least on the detectors 25-32 which are at temperatures below –135°C. This dew point corresponds to water contents in the carrier gas of less than 10 ppb. About 55 % of the Rn is deposited on the detector. Thus, the new COLD device encloses the adsorption range from metallic to Rn-like behaviour of element 112. Experiments to chemically investigate element 112 applying the described set-up are scheduled for February/March 2003 at GSI Darmstadt.

References:

[1] K.S. Pitzer, J. Chem. Phys. 63, 1032 (1975).
[2] B. Eichler, Kernenergie 19, 307 (1976).
[3] C. Düllmann et al., Nucl. Instr. Meth. A479, 631 (2002).
[4] B. Eichler, PSI Bericht Nr. 00-09 (2000).
[5] J.P. Niklaus, diploma thesis Univ. Bern 2003.
[6] B. Eichler et al. J. Phys. Chem. A104, 3126 (2000).

Adsorption of superheavy elements on metal surfaces

C. Sarpe-Tudoran*, V. Pershina**, B. Fricke*, J. Anton*, W.-D. Sepp* and T. Jacob***

*Fachbereich Physik, Universität Kassel, D-34109 Kassel, Germany; **Gesellschaft für Schwerionenforschung, D-64291 Darmstadt, Germany; ***Beckman Institute, CALTECH, Pasadena, 99125, CA, USA

The adsorption of radioactive superheavy nuclei in a thermochromatographic column is one possible method to detect these nuclei and to compare their volatility with known elements. The important physical quantity which controls this process is the binding energy. The theoretical prediction of it is very complicated, but we present here a first ab initio calculation of these quantities for the element 112 and for its homologue Hg on an Au(100) surface. Our main task is to calculate the difference in the adsorption energies between these two elements. We performed the calculations of the binding energies using a relativistic molecular program [1] developed in our group, which solves the relativistic Khon-Sham equations for various density functionals. To solve them the molecular orbitals are taken as a linear combination of atomic orbitals (MO-LCAO).

We employ optimized basis sets obtained from dimer calculations with the same program, which include the additional functions $6p$ and $5f$ for Au and Hg, and $7p$ and $6f$ for element 112. The obtained binding energies (Table 1) differ slightly from those given in [2] because we employed a more extended basis set which included additional nf functions. These results can be interpreted in terms of binding when the surface is approximated by only one atom.

System	Binding energy [eV]		Distance
	rLDA	GGA	[a.u.]
HgAu	–1.03	–0.55	4.9
112Au	–0.93	–0.41	5.0

Table 1: Binding energy and bond distance (rLDA) for the HgAu and 112Au dimers

In our calculations for the adsorption we approximate the surface by moderate clusters (with the number of atoms between 9 and 16). Three possible positions (top, hollow and bridge) of the ad-atom on the cluster are considered. The distances between the atoms of the clusters are kept fixed to their bulk values. In the case of top and hollow positions the C_4v symmetry was used, while the C_2v symmetry was used for the bridge position.

Type of ad-atom	Position of the ad-atom	Binding energy [eV]	Distance [a.u.] to the surface	nearest neighbour
Hg	top	–0.60	5.0	5.0
	bridge	–1.15	4.3	5.1
	hollow	–1.04	3.5	5.2
Element 112	top	–0.67	5.2	5.2
	bridge	–1.08	4.5	5.3
	hollow	–0.99	3.8	5.4

Table 2: Binding energy and bond distances of Hg and element 112 on the Au clusters (rLDA)

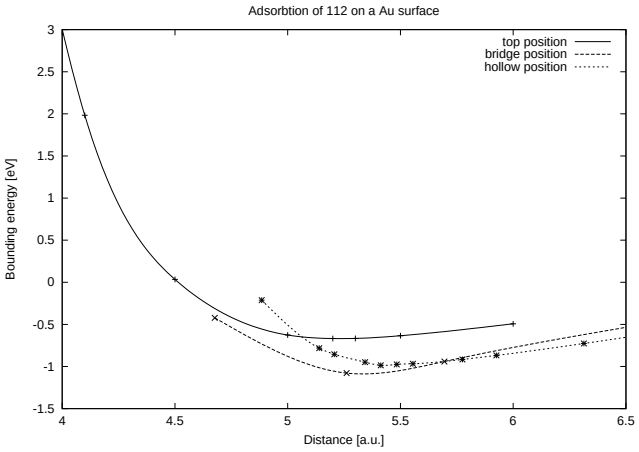

Figure 1: The potential energy curves for the adsorption of element 112 on the Au clusters.

Fig. 1 presents the potential energy curves (rLDA) of element 112 on these three clusters as function of the distance to the nearest neighbours. The values which describe the minima are summarized in Table 2, which also includes the corresponding values for Hg. One can see that for both Hg and element 112 the bridge position on the Au cluster is preferential, with the binding of element 112 being by 0.06 eV weaker than that of Hg.

The values for the top position show the reversed trend from Hg to element 112. This is probably an artifact because the cluster for the top position is too small (only 9 atoms) to lead to good results. Here further calculations with a bigger cluster are necessary. Nevertheless, our experience shows [3] that the bridge position may stay preferential even for larger clusters. Our calculated GGA values for the binding energy of Hg and element 112 on the Au cluster in the bridge position are 0.65 eV and 0.56 eV, respectively. The value for Hg could be compared with the adsorption enthalpy of Hg on the gold surface of -1.01 eV estimated on the basis of experimental data [4]. Results of our calculations suggest that the adsorption enthalpy of element 112 on the Au surface should be about 0.1 eV ($\sim$ 10 kJ/mol) smaller than that of Hg.

References

[1] T. Baştuğ, W-D. Sepp, D. Kolb, G. te Velde, E.J. Baerends, Phys. Rev. B, **28**,(1995) 2325–2331

[2] V. Pershina, T. Bastug, S. Varga und B. Fricke, Chem. Phys. Lett., **365**,(2002) 176–183

[3] T. Jacob, D. Geschke, S. Fritzsche, W.-D. Sepp, B. Fricke, J. Anton, S. Varga, Surf. Sci. **486**, (2001) 194

[4] H. Rossbach, B. Eichler, ZfK-527 Report, Akademie der Wissenschaften der DDR (Juni 1984)

Predictions of adsorption temperature of element 112 on gold for gas-phase chromatography experiments

V. Pershina[1], T. Bastug[2], B. Fricke[3], J. Anton[3]
[1]GSI, Darmstadt; [2]The Australian National University, Canberra
[3]Theoretische Physik, Universität Kassel, Kassel

Investigations of chemical properties of element 112 discovered by the GSI laboratory, Darmstadt, are to be conducted by an international collaboration of several experimental groups [1,2]. Element 112, the heaviest man-made transition d-element, is expected to exhibit an unusual chemical behaviour due to the maximum of relativistic effects on the 7s orbital shell in the 7th row of the Periodic Table: Due to the very strong relativistic contraction and stabilization of the 7s electrons and its closed shell ground state configuration, $7s^26d^{10}$, element 112 is expected to be almost as inert as a noble gas and, therefore, volatile.

In view of coming experiments, predictions of adsorption of element 112 on metal surfaces based on quantum-chemical calculations are highly desirable. As a first step in such a study, bonding in the dimers MHg and M112, where M=Pd, Cu, Ag and Au, has been determined using the four-component relativistic density-functional theory method (RDFT) [3]. First calculations of the interaction of Hg and element 112 with small clusters of the above mentioned metals have also meanwhile been reported by our groups [4]. In the present work, a way is suggested to predict the adsorption temperature of an element (in this case of element 112) using thermodynamic equations for the adsorption equilibrium.

In the isothermal chromatography an adsorption temperature, T_{ads}, of a heaviest element (B) in relation to that of its lighter homolog (A) at the established adsorption-desorption equilibrium (the peak of the temperature distribution curve) is usually measured. This corresponds to the condition when $K_A(T_A) = K_B(T_B)$, or using statistical thermodynamics

$$e^{-\Delta E_A / RT_A} \frac{Q_A^s}{Q_A^g} = e^{-\Delta E_B / RT_B} \frac{Q_B^s}{Q_B^g}, \qquad (1)$$

where ΔE is the adsorption energy of a species A or B, and Q is their partition function. Due to a model of localized adsorption, where an atom is considered to be bound to the surface and the contribution of the configurational entropy should be taken into account, the equilibrium constant is

$$K = \frac{Q_{conf}^s Q_{vibr}^s}{Q_{trans}^g Q_{rot}^g} \qquad (2)$$

Since experiments for the heaviest elements and their homologs are conducted in the same set up under the same conditions and often simultaneously, any parameter on the left- and right-hand sides of eq. (1) connected with specific experimental conditions cancel, so that the final equation depends only on properties of the adsorbate and on its interaction with the adsorbent, i.e.

$$e^{-\Delta E_A / RT_A}\left(\frac{\pi IR_A^2}{d^2}-1\right)\frac{T_A^{3/2}}{\nu_A^3 r_A^3 m_A^{3/2}} = e^{-\Delta E_B / RT_B}\left(\frac{\pi IR_B^2}{d^2}-1\right)\frac{T_B^{3/2}}{\nu_B^3 r_B^3 m_B^{3/2}} \qquad (3)$$

Here m is the mass of a species, IR its ionic radius upon an interaction with the surface, r is atomic radius of the gaseous species, d is the distance between atoms in a metal lattice of the adsorbent, and ν is a vibration frequency of the adsorption bond. Using eq. (3), either adsorption temperature of a species can be defined on the basis of the knowledge of its interaction with the surface, or its sublimation enthalpy can be determined from its adsorption temperature, provided T_{ads} and ΔH_{ads} are known for a homologous one. The r values for Hg and element 112 have been, and those for IR can be calculated using the atomic relativistic Dirac-Fock method [5] (Table 1).

Table 1. Properties of Hg and element 112 used for the calculations of T_{ads} of element 112

Property	Hg	112	Comment
$r_{A/B}$, Å	1.815	1.711	r_{Hg} - Δr_{max}(Hg/112)
IR(Hg/112-ads.), Å	1.36	1.41	from calc. R_e [3]
$m_{Hg/112}$, g/at	186	283	used in experiments
$\nu_0 \cdot 10^{-12}$, s^{-1}	2.99	2.21	calculated [3]

To give T_{ads}(112) relative to the experimental T_{ads}(Hg), ΔE_{ads}(112) is taken as "experimental" ΔH_{ads}(Hg) (deduced using the Monte-Carlo simulation from an experimental T_A, e.g., of 155 °C [2]) minus the calculated difference in the binding energies of 21.7 kJ/mol between the dimers HgAu and 112Au. The solution of eq. (3) with parameters of Table 1 gives a difference in T_{ads} between Hg and element 112 of 96 degrees. Thus, results of our DFT calculations for the dimers suggest that element 112 should form metal-metal bonding and should be adsorbed at a much higher temperature than that of Rn. This should, however, take place at ideal circumstances (for which the calculations were performed): any deviation from an ideal surface/lattice would result in the formation of the van der Waals bond and a shift of T_{ads} of element 112 in the area of T_{ads} of Rn.

References

[1] H. W. Gäggeler, *et al.*, GSI Proposal 2002.
[2] J.-P. Niklaus, *et al.*, PSI Annual Report 2002, p. 8.
[3] V. Pershina, *et al.*, Chem. Phys. Lett. **36**, 176 (2002).
[4] C. Sarpe-Tudoran, *et al.*, GSI report 2002, this issue.
[5] J.-P. Desclaux, At. Data Nucl. Data Tabl. **12**, 311 (1973).

Theoretical Treatment of Complexation of Element 106, Sg, in HF Solutions

V. Pershina[1] and J. V. Kratz[2]
[1]GSI, Darmstadt
[2]Institut für Kernchemie, Universität Mainz, 55099 Mainz

The first chemical study of seaborgium in aqueous solution was its one-step elution as a neutral or anionic species in 0.1 M HNO_3/$5\cdot10^{-4}$ M HF from cation exchange columns [1]. These experiments showed the most stable oxidation state in aqueous solutions to be +6 as expected for a member of group-6 elements. In future experiments with ^{265}Sg it was planned to determine K_d-values on an anion exchanger in HF/0.1 M HNO_3 solutions using on-line chromatography and the multi-column technique. First measurements for batch and ARCA experiments for Mo and W, homologs of Sg, in HF/HNO_3 solutions were reported [2,3]. The results have shown a complex dependence of K_d on the HF concentration due to a competition between the complex formation and hydrolysis of group-6 elements.

To render assistance to this experimental work and predict extraction behaviour of Sg in future experiments, complex formation and hydrolysis of Mo, W, and Sg were considered theoretically on the basis of relativistic calculations for various hydrated, hydrolyzed and fluoride complexes. The free energy change for the following fluorination process

$$MoO_4^{2-} \Leftrightarrow MO_3F^- \Leftrightarrow MO_2(OH)_2F_2 \Leftrightarrow$$

$$MO_2F_3(H_2O)^- \Leftrightarrow MO_2F_4^{2-} \Leftrightarrow MOF_5^-$$

has been defined for Mo, W, and Sg using a model [4]. This model enables determination of the changes in the ionic and covalent contributions to the total binding energy using the Mulliken population analysis of the electronic density distribution. The latter was calculated using the fully relativistic Density-Functional method [5]. The geometry of the molecules was estimated from experimental or extrapolated ionic radii.

As a result of the calculations, changes in the Coulomb part of the free energy for the fluorination process indicated above at different pH have been obtained as given in Tables 1 and 2.

Table 1. Changes in the Coulomb part of the free energy ΔE^C (in eV) for the fluorination reactions at pH < 1

Reaction	Mo	W	Sg
$MO(OH)_3(H_2O)_2^+ \Leftrightarrow MO_3F^-$	27.48	28.34	28.32
$MO(OH)_3(H_2O)_2^+ \Leftrightarrow MO_2F_2(H_2O)_2$	10.56	11.04	11.34
$MO(OH)_3(H_2O)_2^+ \Leftrightarrow MOF_3(H_2O)^-$	20.15	20.27	21.66
$MO(OH)_3(H_2O)_2^+ \Leftrightarrow MOF_5^-$	21.83	21.54	21.06

The obtained values of ΔE^C show a very complicated dependence of the complex formation sequence in the group depending on a sort of reaction, i.e. on the HF concentration and pH. Generally, the trends can be summarized as it is shown in Table 3.

Table 2. Changes in the Coulomb part of the free energy ΔE^C (in eV) for the fluorination reactions at pH > 1

Reaction	Mo	W	Sg
$MO_4^{2-} \Leftrightarrow MO_3F^-$	-10.98	-11.13	-11.06
$MoO_3(OH)^- \Leftrightarrow MO_3F^-$	2.01	1.99	1.89
$MoO_3(OH)^- \Leftrightarrow MO_2F_2(H_2O)_2$	-14.23	-14.52	-14.29
$MoO_2(OH)_2(H_2O)_2 \Leftrightarrow MO_2F_2(H_2O)_2$	5.43	5.47	5.45
$MoO_2(OH)_2(H_2O)_2 \Leftrightarrow MO_2F_3(H_2O)^-$	15.39	15.09	15.17
$MoO_2(OH)_2(H_2O)_2 \Leftrightarrow MO_2F_4^{2-}$	27.36	26.63	26.57
$MoO_2(OH)_2(H_2O)_2 \Leftrightarrow MO_2F_5^-$	18.08	17.60	17.11

Table 3. Trends in the formation of various fluoride complexes of Mo, W, and Sg depending on pH and type of complex

Complex	Trend
pH >1	
MO_3F^-	W > Mo > Sg
$MO_2F_2(H_2O)_2$	Mo > Sg > W
$MOF_3(H_2O)^-$, MOF_5^-	Sg > W > Mo
pH < 1	
MO_3F^-	Mo > Sg ≥ W
$MO_2F_2(H_2O)_2$	Mo ≥ Sg > W
$MOF_3(H_2O)^-$	Mo > W > Sg
MOF_5^-	Sg > W > Mo

If the experiment with Sg will be conducted in the 0.1 M HNO_3, the situation will be even more complex as it is shown in Table 3. One can expect, however, that at very low HF concentrations, [HF] < 10^{-5} M, the sequence in the K_d values in the anion exchange separations will be W > Sg > Mo. In the middle range, 10^{-5} < [HF] < 10^{-1} M, it will be very probably Mo > Sg > W, while at the high [HF] >> 10^{-1} M, Sg will be much better extracted than Mo and W: Sg >> W > Mo. In the full publication on this subject, the relations in K_d values between Mo, W, and Sg will be also given. The predicted sequences (Table 3) are in agreement with those obtained experimentally for Mo and W [2]. This is a good indication that Sg will be observed as predicted. The best separation of Sg from Mo and W can be expected at [HF] > 1 M.

References

[1] M. Schädel, *et al.*, *Nature* **388**, 55 (1997).
[2] A. Konenberg, *et al.*, GSI Annual Report 1999, p. 238.
[3] A. Kronenberg, Doctoral Thesis, Mainz, 2001.
[4] V. Pershina, *Radiochim. Acta* **80**, 65 (1998).
[5] T. Bastug, *et al*., *Chem. Phys. Lett.* **211**, 119 (1993).

Reduction of Mo(VI) in ALOHA

B. Wlodzimirska[1*], K. Eberhardt[1], J.V. Kratz[1], S. Zauner[1], W. Brüchle[2], E. Jäger[2], M. Schädel[2], E. Schimpf[2]
[1]Institut für Kernchemie, Universität Mainz, [2]Gesellschaft für Schwerionenforschung, Darmstadt

In previous studies, tungsten (W) and molybdenum (Mo), the homologs of seaborgium (Sg), were used to develop a reduction experiment in which, for the first time, a transactinide element is attempted to be reduced to a lower oxidation state [1,2]. It had been shown theoretically, that reduction of Sg(VI) to Sg(III) should be feasible with a strongly reducing metal such as Al [3]. Accordingly, Strub et al. [1,2] studied reduction of W and Mo in 0.1 M HCl/0.1 M HF in a heterogeneous system with Al metal at a solution temperature of 80° C. Even though it could be shown that reduction of W and Mo was possible in principle, the distinction of M(III) from M(VI) on an anion-exchange column (1.6 x 8 mm) was unsatisfactory. (M(III) is supposed to be eluted immediately from the anion-exchange column while M(VI) is expected to be sorbed on the resin. Unfortunately, with the small-size columns of the ARCA type, a sufficient retention of M(VI) on the anion-exchange column was never achieved [1,2].

As an alternative to the discontinuous ion-exchange chromatography with ARCA, Kronenberg et al. [4] developed an on-line chromatography with the multi-column technique combined with the quasi-continuously working gas-jet collection system ALOHA. We have installed this system at the TRIGA reactor, see Fig. 1. A ^{235}U target covered with 15 µm Al to suppress the heavy-mass fission products was irradiated with neutrons and the light-mass fission products were stopped in He gas containing KCl aerosols. At a flow rate of 2 L/min, the activity bearing aerosols were transported from the target chamber through a 1.5 mm i.d. capillary to ALOHA were the aerosol was deposited on a Ta disc by impaction. The deposited KCl was dissolved in mixed HCl/HF solutions of different molarities and the solution was pumped at 1 mL/min through three columns. The first one served as filter column F [4] and was filled with 67 mg of the cation-exchange resin AG 50Wx8. The second one contained in a narrow bore an Al wire of 58 mm length heated to 80° C.
The third one was identical with column F. Mo(VI) passing the column F as anionic fluoride complex, was reduced in contact with the Al, and the reduced species was sorbed in the third column. Variation of the molarity of the mixed HCl/HF solutions showed that optimum yields were obtained with 0.001 M HCl/0.01 M HF. Yields of dissolution in ALOHA including the yield of impaction were about 90 %. The yield of reduction and the retention of the reduced Mo on the third column was nearly quantitative. The amount of Al dissolved per mL of 0.001 M HCl/0.01 M HF was 0.061 mg. On the cation-exchange columns used for the recovery of ^{253}Es, the long-lived descendant of ^{265}Sg, the dissolved Al does not present a problem as it is eluted as fluoride complex, i.e., the capacity of the cation-exchange columns is not limited by the dissolved Al.

In summary, the problems encountered in previous versions of the reduction experiment in group 6 have been solved so that the experiment with Sg can be envisaged.

References

[1] E. Strub et la., Jahresbericht 1999, IKMz 2000-1, A11
[2] E. Strub, Doctoral disseration, Mainz (2000)
[3] V. Pershina et al., J. Phys. Chem. A **103**, 8463 (1999)
[4] A. Kronenberg et al., Jahresbericht 2001, IKMz 2002-1, A4

*on leave from Institute of Nuclear Chemistry and Technology, Warsaw, with a fellowship of IAEA

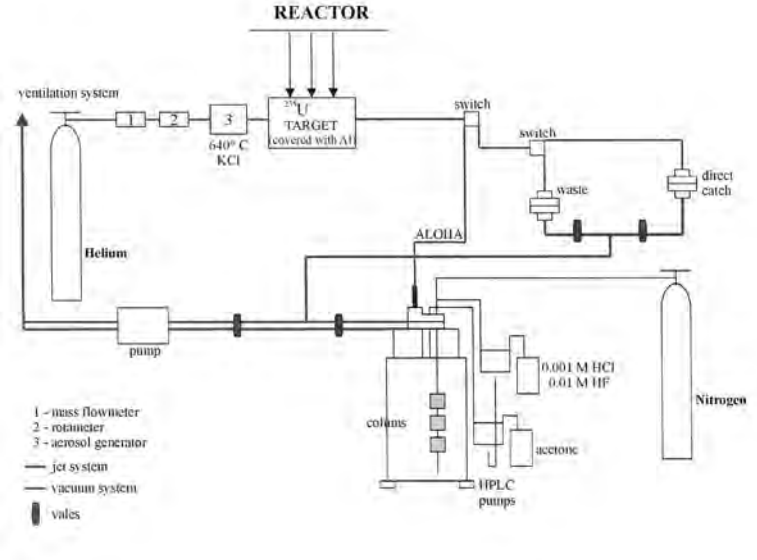

Fig. 1: Schematic of the equipment

Electrodeposition of Po-210 on various electrode materials

U. Rieth, H. Hummrich, J.V. Kratz
Institut für Kernchemie, Johannes Gutenberg-Universität Mainz, D-55099 Mainz

For future investigation of the chemical properties of superheavy elements, the spontanous electrodeposition of carrierfree polonium is beeing studied.
In a first preparatory step, the polonium tracer was produced at the Mainz TRIGA reactor by irradiating natural bismuth. After the Bi-210 ($T_{1/2}$=5d) reached its radiochemical equilibrium with Po-210 ($T_{1/2}$=138d) the elements were separated by anion-exchange chromatography using the Biorad AG MP-1 (100-200mesh) exchange resin [1]. A conc. HCl solution of the Bi-210/Po-210 was fed onto the exchange column (d=13mm, h=50mm). After elution of the Bi fraction with 100ml conc. HCl (flowrate 1.5ml/min), the carrierfree Po-210 could be eluted from the column with 300ml HNO_3 (1:1) (flowrate 1.5ml/min) as shown in Fig.1.

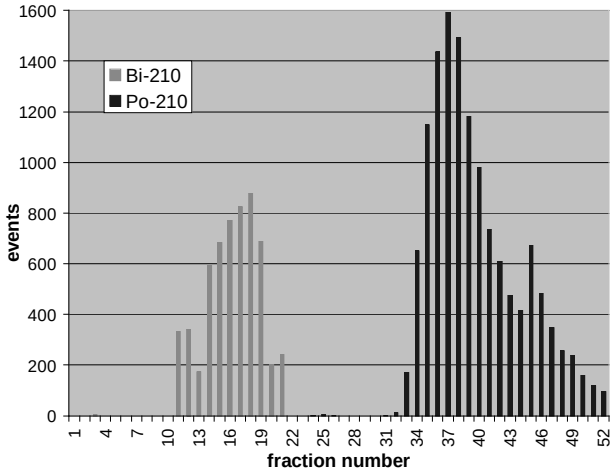

Fig.1 Elution of Bi-210 and Po-210 from the anion-exchange column AG MP-1.

To get a Po-210 solution usable in electrochemical experiments, the fractions containing Po are evaporated to dryness and are dissolved in the desired solvent afterwards.

Reproducible results in electrochemical experiments can only be achieved by using electrodes with very clean surfaces. To get such electrodes, a procedure was established, where the electrodes (metal foils) are cleaned in a three-step process. First, the foils are washed in acetone to remove grease.

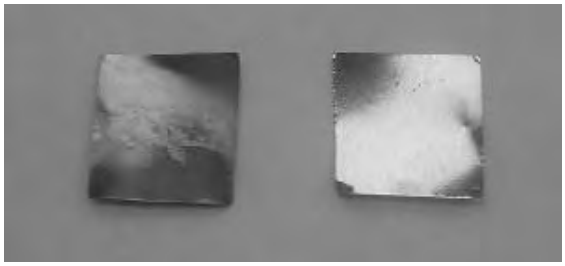

Fig.2 Cu electrodes prior and after the surface cleaning.

In a second step, the electrodes are heated under an argon/hydrogen (95:5) atmosphere at about 700K for 2 hours to remove oxide species from the surface. In a final step, the adsorbed layer of hydrogen is removed by a heat treatment at 400-500K under a pure argon atmosphere or by another heating process under vacuum conditions. Fig.2 illustrates the change in optical appearance of a copper-foil electrode prior and after the treatment.

Using a 0.1M HNO_3 solution of Po-210, a first series of experiments on the spontanous electrodeposition of Po has been performed. These experiments used Cu, Ag, Ti, Pd and Ni in form of 6x6mm foils as electrode materials. These foils were introduced into a small electrochemical cell with a volume of only 200µl [2]. After contacting the electrode with the Po-210 electrolyte, the reaction time was started. To assure a maximum ion motion towards the electrode, the cell was heated to 340K and treated with ultrasound. In these first experiments, a very long reaction time of 15min was chosen. At the end of the reaction, the elctrode was removed from the cell and rinsed with water to stop all reactions. The determination of the amount of deposited Po was performed by alpha spectroscopy. Fig.3 shows the results for the various electrode materials.

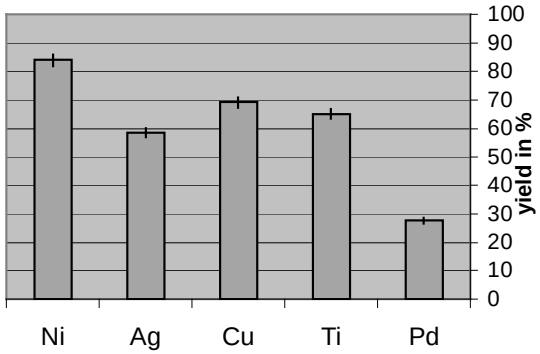

Fig.3 Deposition yields of Po-210 on metal foils.

It can be noticed that the deposition of Po on a Pd electrode is very inefficient. This is in contradiction to a theoretical prediction by Eichler et al. [3]. As that prediction is only valid for a very low surface coverage of only a single monolayer, the degree of coverage was calculated using the experimental parameters (electrode surface area, activity of the electrolyte). The calculations resulted in a coverage of $7*10^{-6}$% which is well within the monolayer limit.
Because of the relatively good deposition results observed with Ni, Cu and Ag, future experiments will be performed using these materials. In the planned experiments, the first goal must be to reduce the deposition time by at least an order of magnitude. This has to be achieved with respect to the half lives of the superheavy elements which are to be investigated using this electrochemical technique.

References

[1] J. Korkisch, *Handbook of Ion Exchange Resins: Their Application to Inorganic Analytical Chemistry*, Volume VI, CRC Press, Boca Raton (1989)

[2] U.Rieth et al., Institut für Kernchemie der Universität Mainz, *Jahresbericht 2001*, A12.

[3] B. Eichler, J.V. Kratz, *Radiochim. Acta* **88**, 475 (2000).

The critical potential of the Pb underpotential deposition (UPD) on Pt

H. Hummrich[1], U. Rieth[1], J.V. Kratz[1], B. Eichler[2]
[1]Institut für Kernchemie, Universität Mainz; [2]PSI Villigen

The electrodeposition of a metal ion A^{n+} on a foreign metal surface B in the sub-monolayer region often takes place at a more positive potential compared to the potential calculated via the Nernst equation. The so called underpotential deposition has been studied by cyclovoltammetry [1] and radiotracer methods [2]. Calculations with a modified Nernst equation basing on physical properties of the deposited and the electrode metal lead to predictions for electrode potentials for the deposition of 50% of A^{n+} on B ($E_{50\%}$-values). $E_{50\%}$-values were calculated for the deposition of element 112 to 115 and their homologues Hg, Tl, Pb and Bi on noble metals such as Au, Pt and Pd [3],[4]. According to these predictions it might be possible to perform electrodeposition experiments with element 114. To verify the predictions, more experimental data are necessary. Hevesy and Paneth defined the critical potential E_{crit} as the potential, at which electrodeposition of a radiotracer on a metal electrode first occurs [5]. Obviously, critical potentials measured in an experiment should be similar to the predicted $E_{50\%}$ values.

Tab.1 Predicted E50% values (vs. Ag/AgCl (3M KCl) electrode) for the deposition of Pb and element 114 on noble metals [3,4]

Electrode	Cu	Pd	Ag	Pt	Au
Ion					
Pb^{2+}	-0,52	0,31	-0,47	0,01	-0,40
114^{2+}	1,04	0,66	0,74	1,14	0,64

We carried out deposition experiments with ^{212}Pb as radiotracer. As electrode metal we chose Pt. ^{212}Pb was prepared by using a ^{220}Rn emanating source (^{228}Th co-precipitated with Zr-Stearate). The ^{220}Rn daughter products were collected from the gas phase on a Pt-electrode at a potential of -150V for 24h. ^{212}Pb was then dissolved with hot 6 N HCl, the solution was evaporated to dryness and dissolved in 0,1 N HCl.

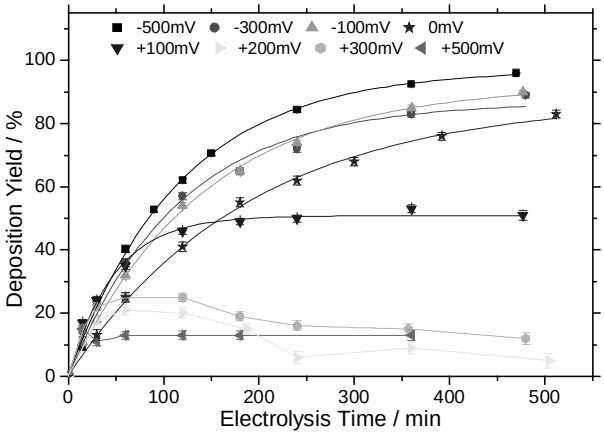

Fig.1 Electrodeposition of ^{212}Pb on a Pt electrode vs. electrolysis time at different electrode potentials (vs. Ag/AgCl, 3M KCl)

The deposition experiments were performed at constant electrode potentials, see Fig.1, by using a potentiastatic three-electrode system with a Ag/AgCl (3M KCl) reference electrode, a Pt working electrode and a Pt counter electrode. The area of the working electrode was 2 cm², the total volume of the solution was 20 ml, for agitation a constant nitrogen flow was applied. Prior to the experiment, the working electrode was cleaned at +1400mV for 15 min.

To determine the deposition of ^{212}Pb vs. the electrodeposition time without disturbing the system, we measured the decrease of the activity in the solution. This experiment was repeated at different electrode potentials. The experimental data were fitted by equation (1).

$$\frac{N_{dep}}{N_{tot}} = \frac{a}{a+b} - \frac{a}{a+b} \cdot e^{-(a+b)\cdot t} \qquad (1)$$

N_{dep} is the amount of deposited atoms, N_{tot} is the total amount. The term a/(a+b) represents the maximum deposition yield for a given electrode potential. The critical potential determined with Joliot's method (Fig. 2) [2] is +190 mV, this is in good accordance with the critical potential of +255 mV for the deposition of Pb on Pt in 1 N HNO_3 measured by Ziv et al. [6]. The predicted $E_{50\%}$ value (+10 mV) is somewhat lower than the measured E_{crit}-value, but the difference gets smaller if compared with the potential at which the maximum deposition yield is 50% (approx. +100mV).

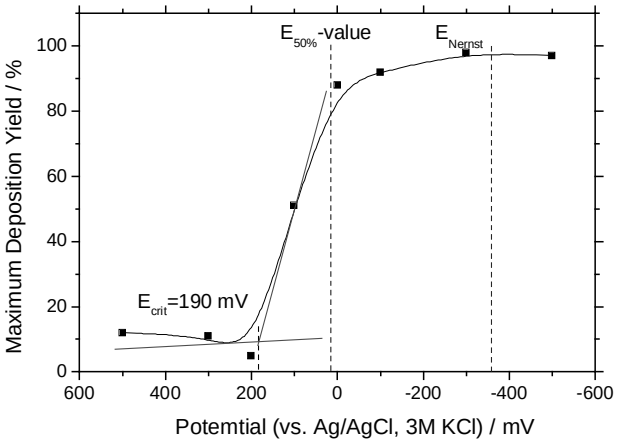

Fig.2 Determination of the critical potential E_{crit} for the deposition of ^{212}Pb on Pt in 0,1 N HCl (vs. Ag/AgCl 3M KCl)

The use micro-reference electrodes (0,5-1,5 mm diameter) will allow experiments with small volumes (100µl). This should lead to a drastic decrease in electrodeposition time. Future plans are to develop an automated apparatus for electrodeposition experiments with superheavy elements.

References

[1] D.M Kolb, M. Przasnyski, H. Gerischer, J. Electroanal. Chem. **54,** 25 (1974)
[2] F. Joliot, J. Chim. Phys. **27,** 119 (1930)
[3] B. Eichler, J.V. Kratz, Radiochimica Acta **88,** 475 (2000)
[4] B. Eichler, H. Rossbach, GSI-tr-89-17 (1989)
[5] G.v. Hevesy, F. Paneth, Monatshefte **36,** 45 (1915)
[6] D.M. Ziv, G.M. Sukhodolov, V.F. Fateev, L.I. Lastochin, Radiochemistry **8,** 182 (1966)

Background free α-LSC spectra with the help of neural networks

G. Langrock, N. Wiehl, K. Eberhardt, H.O. Kling, M. Mendel, A. Nähler, U. Tharun,
N. Trautmann, J.V. Kratz
Institut für Kernchemie, Universität Mainz

Liquid scintillation counting (LSC) is based on the excitation of a solution of mostly organic substances by an ionizing particle leading to the emission of a light pulse. This light pulse has a characteristic shape depending on the type of particle. Conventional methods for the differentiation of the different pulse shapes are based on analog pulse - shape discrimination (PSD). However, these PSD units fail in the case of high numbers of background events and when unusual pulse shapes occur.

An alternative is digital recording of scintillation pulses with the help of so-called transient recorders and a subsequent off line pulse - shape discrimination with the help of artificial neural networks. The stepwise developement of this method has been described earlier [1,2] in connection with experiments with the fast liquid-liquid extraction system SISAK performed to study the chemical properties of rutherfordium (Rf). These experiments showed that Rf α decays could not unambiguously be distinguished from β–/γ events and pile ups by the analog electronics used. The evaluation described in [2] of an experiment performed in February 2000 at the Paul-Scherrer Institute (PSI, Villigen) showed that the ansatz of a pulse-shape discrimination with neural networks (PSD-NN) is functioning in principle, but could be improved in detail.

Several parameters were changed. The newly adopted neural net that had been trained with 2580 scintillation pulses, consisted of three layers. The entrance layer contained 175 neurons (corresponding to a pulse with 175 data points à 2 ns), the second layer contained 5 neurons, and the exit layer 2 neurons. The output of the latter delivered, with values between 0 and 1, a reliable information about the character of the pulses (α yes or no). Compared to the net described previously [2], two principal changes were realized. Firstly, all pulse heights were normalized to one for the evaluation with the neural network. Secondly, in the ascending flank of each pulse, a start point was defined, from where on the 175 data points of the pulse are recorded. These changes lead to a drastically improved recognition performance of the neural net, see Fig. 1. As an example, Fig. 1 shows a LSC spectrum containing all registered events , as well as a spectrum containing only pulses that the neural net had automatically classified as α pulses. This spectrum does no longer contain any background events.

For a complete analysis of the SISAK experiment of February 2000, a search for ^{261}Rf – ^{257}No

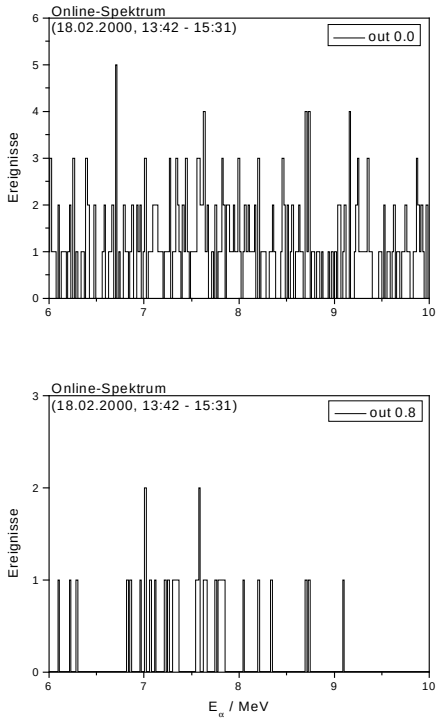

Fig. 1: α-LSC spectra from a SISAK experiment performed in February 2000. The original spectrum (output value 0.0) is shown on the top, the spectrum after automatic removal of background events (output value 0.8) by the neural network is shown below.

αα correlations within an energy window between E_α=7.7 and 8.8 MeV was performed. Two αα correlations were found [3]. This small number of events is primarily related to a bad performance of the He (KCl) jet. Insofar, statements related to the chemistry of rutherfordium cannot be deduced from this experiment.

In summary, an empirical method has been established with the help of which background free LSC spectra can be obtained. This opens new possibilities for different kinds of low – level measurements in nuclear and radiochemistry.

[1] G. Langrock et al., Institut für Kernchemie, Universität Mainz, Jahresbericht 2000, IKMz 2001 – 1, A7
[2] G. Langrock et al., Institut für Kernchemie, Universität Mainz, Jahresbericht 2001, IKMz 2002 – 1, A8
[3] G. Langrock, Doctoral dissertation, Universität Mainz (2002)

Beta-decay studies of neutron-deficient Sn isotopes

M. Karny[1], Z. Janas[1], L. Batist[2], J. Döring[3], I. Mukha[3], C. Plettner[3], A. Banu[3], A. Blazhev[3], F. Becker[3], W. Brüchle[3], T. Faestermann[4], M. Górska[3], H. Grawe[3], A. Jungclaus[5], M. Kavatsyuk[3], O. Kavatsyuk[3], R. Kirchner[3], M. La Commara[6], S. Mandal[3], C. Mazzocchi[3], A. Płochocki[1], E. Roeckl[3], M. Romoli[7], M. Schädel[3], R. Schwengner[8] and J. Żylicz[1]

[1]University of Warsaw, Poland; [2]St. Petersburg Nuclear Physics Institute, Russia; [3]GSI, Darmstadt, Germany; [4]Technische Universität München, Germany; [5]IEM CSIC, and Universidad Autónoma de Madrid, Spain; [6]Universitá di Napoli, Italy; [7]INFN Napoli, Italy; [8]Forschungszentrum Rossendorf, Germany

Studies of nuclei in the ^{100}Sn region offer the possibility to test nuclear models describing structure and decay properties of nuclei in which protons and neutrons occupy identical orbitals near a double shell closure. An insight into the structure of nuclei close to ^{100}Sn can be gained by studying their β decay which is dominated by $\pi g_{9/2} \rightarrow \nu g_{7/2}$ Gamow-Teller (GT) transitions. An attractive feature of such nuclei is that most of the GT strength lies within the Q_{EC}-value window. Such a concentration of strength has recently been observed in a series of light indium and silver isotopes (see [1] and references therein). ^{100}Sn has been predicted to decay by one GT transition to a single 1^+ 1p-1h state in ^{100}In at an excitation energy of about 1.8 MeV, while the closest even-even neighbours of ^{100}Sn, ^{98}Cd and ^{102}Sn, show a spreading of the GT strength over a number of 1^+ states in the daughter nucleus.

In the recent experiments at the GSI-ISOL facility we used the FEBIAD-B3C ion sources with the addition of CS_2 [2] for the mass separation of SnS^+ ions. In this way routinely about 60% of the intensity of the Sn^+ beam was shifted to the SnS^+ molecular side-band, where the strong suppression of contaminants [2] cleaned the beams from In, Cd, and Pd isobars. Only the strongly produced activities of Ag were traced in on-line experiments, the suppression of which was 4-5 times lower than the anticipated value of 10^4 found in off-line studies. The latter effect may be due to an operation of the ion source at lower temperature compared to the off-line measurement, which was made to enhance the SnS^+ intensity. We measured β-γ-γ decay properties of $^{101-105}$Sn with two complementary set-ups, namely (i) the Total Absorption Spectrometer (TAS) for the measurement of GT strength distributions and (ii) an array of germanium detectors (including a FZR-Cluster and two GSI-Clover detectors) operated in coincidence with silicon β-detectors. β-delayed protons of ^{101}Sn were measured by using ΔE-E silicon telescopes. The intensities of the mass-separated $^{101-105}$Sn beams were obtained from the experimental decay properties. By using a 40 particle-nA ^{58}Ni beam, a 3 mg/cm^2 ^{50}Cr target, and a catcher of ZrO_2 fibers inside the FEBIAD source, we reached secondary beam intensities given in Table 1. These values are about one to two orders of magnitude higher than those obtained by a previous FRS experiment [3].

The data on the ^{102}Sn decay collected with the high resolution set-up (ii) as well as spectra obtained by the small germanium detector in the TAS confirm the main features of the ^{102}Sn decay scheme proposed by Stolz [3] on the basis of an FRS experiment. The main difference is that we do not confirm the 53 keV transition (see Fig. 1), which was previously [3] placed at the very bottom of the ^{102}In level scheme. Removing this transition from the decay scheme may affect the spin assignment of the ground state of ^{102}In. Figure 2 presents the β-gated TAS spectrum of ^{102}Sn after subtraction of contributions from daughter activities which were determined in separate measurements. The maximum occurring at a recorded TAS-energy of about 2.5 MeV is interpreted as being due to the $\pi g_{9/2} \rightarrow \nu g_{7/2}$ GT resonance at a ^{102}In excitation energy of about 1.5 MeV.

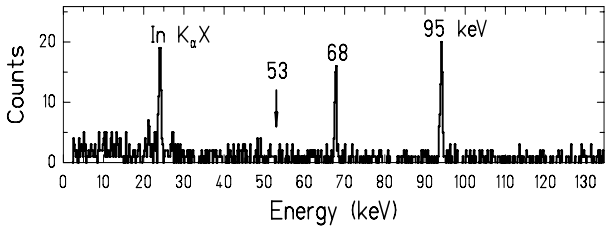

Figure 1: Low energy γ-ray spectrum obtained for mass 102. An arrow shows the expected position of the 53 keV line which remained unobserved in this experiment.

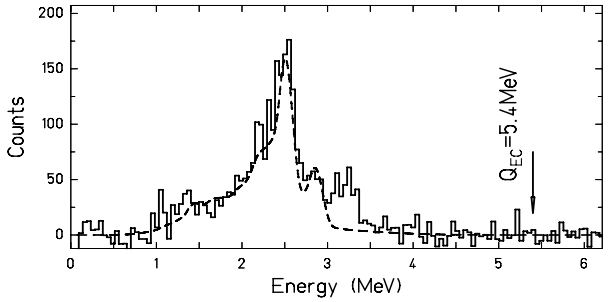

Figure 2: Beta-gated TAS spectrum of ^{102}Sn from the experiment (solid line) and from a GEANT simulation based on the modified level scheme of Ref. [3] (dashed line).

In summary, the development of SnS^+ beams at the GSI ISOL allowed us to study in detail the β-decay properties of $^{101-105}$Sn. These data, in particular those on β-γ-γ coincidences, are under evaluation. An extrapolation of the experimental beam intensities, yields 8 atoms/h for ^{100}Sn indicating that the measurement of β-delayed γ rays of this nucleus will indeed be a very challenging task.

References

[1] C. Plettner *et al.*, Phys. Rev. **C66,** 044319 (2002)

[2] R. Kirchner, Nucl. Instr. and Meth. B, in print, and www.gsi.de/annrep2001 (page 211)

[3] A. Stolz, Ph.D. Thesis, TU München (2001)

Table 1: Measured ISOL rates of the $^{101-105}$Sn isotopes.

Isotope	^{101}Sn	^{102}Sn	^{103}Sn	^{104}Sn	^{105}Sn
atoms/min	2.4	31	$1.4 \cdot 10^3$	$3.0 \cdot 10^4$	$2.0 \cdot 10^5$

Beta decay of ^{103}Sn

O. Kavatsyuk[1,2], M. Kavatsyuk[1,2], J. Döring[1], L. Batist[3], A. Banu[1], F. Becker[1], A. Blazhev[1,4], W. Brüchle[1], T. Faestermann[5], M. Górska[1], H. Grawe[1], Z. Janas[6], A. Jungclaus[7], M. Karny[6], R. Kirchner[1], M. La Commara[8], S. Mandal[1], C. Mazzocchi[1], I. Mukha[1], C. Plettner[1], A. Płochocki[4], E. Roeckl[1], M. Romoli[8], M. Schädel[1], R. Schwengner[9] and J. Żylicz[6]

[1]GSI, Darmstadt, Germany; [2]Kiev National University, Ukraine; [3]St. Petersburg Nuclear Physics Institute, Russia; [4]University of Sofia, Bulgaria; [5]Technische Universität München, Germany; [6]University of Warsaw, Poland; [7]Instituto Estructura de la Materia, CSIC, and Departamento de Fisica Teórica, UAM Madrid, Spain; [8]Universitá di Napoli, Italy; [9]Forschungszentrum Rossendorf, Germany

Doubly closed-shell nuclei and neighbouring isotopes/isotones provide a sensitive test ground for the nuclear shell model. ^{100}Sn is the heaviest doubly-magic N=Z nucleus, located at the proton drip line, where protons and neutrons occupy identical shell-model orbitals. The overlap of their wave functions is large, which further causes a strong proton-neutron interaction to be expected. Beta decay in this region is dominated by an allowed Gamow-Teller (GT) transformation $\pi g_{9/2} \rightarrow \nu g_{7/2}$, which in the decay of an even-even nucleus populates the $I^{\pi} = 1^{+}$ GT resonance. For an odd-neutron parent nucleus the coupling of this resonance to the unpaired nucleon can be studied. This provides a test of the residual interaction via the β-delayed γ-ray spectroscopy.

Measurements of β-delayed γ-rays and protons were performed at the GSI-ISOL facility for ^{101,103,105}Sn. It was essential for this experiment to efficiently suppress the isobaric indium, cadmium, silver and palladium contaminants by using the novel sulphurisation technique [1]. The β-delayed γ-ray spectra were measured with an array of high-resolution germanium detectors (17 crystals) in grow-in mode as well as with the Total Absorption Spectrometer (TAS) in decay mode. Moreover, ΔE-E telescope was used to record β-delayed protons [2, 3]. Further experimental details are given in refs. [1-3].

We report on the new data for the β decay of ^{103}Sn. In Fig. 1 the β-gated γ-ray spectrum for ^{103}Sn, taken at mass A=103+32 with the germanium array, is shown. The 720, 726 and 740 keV lines are known to belong to the decay of the ^{103}In daughter activity [4]. The 1077 keV line has been identified by in-beam spectroscopy [5] to represent the $11/2^{+} \rightarrow 9/2^{+}$ transition in ^{103}In. The data shown in Fig. 1 yield the first evidence for β-delayed γ-rays of 643, 821, 1077, 1356, 1397 and 1428 keV, which are preliminarily assigned to the decay of ^{103}Sn. The TAS spectrum gated by protons is shown in Fig. 2. The 776 and 776+1022 keV lines correspond to the 2^{+} state in ^{102}Cd fed by β-delayed protons after a EC and β^{+}-decay of ^{103}Sn, respectively. Based on these data, a β^{+}/EC ratio of 0.06 for the proton emission to the 2^{+} state in ^{102}Cd was estimated. A corresponding ratio of 0.6 for the proton emission to the ground state in ^{102}Cd was obtained using a proton-γ anti-coincidence condition. The Q_{EC} value of ^{103}Sn was preliminarily determined from these β^{+}/EC ratios and the average energy of β-delayed protons [6] to be 7.5±0.5 MeV.

The half-life of ^{103}Sn, obtained from the β-delayed proton time distribution, is shown in the inset of Fig. 2. The result of the fit being $T_{1/2} = 7.0 \pm 0.6$ s is in agreement with the previously measured values of 7±3 s [6], 7.5±1.5 s [7] and in disagreement with 8.7±0.6 s [8] by two standard deviations.

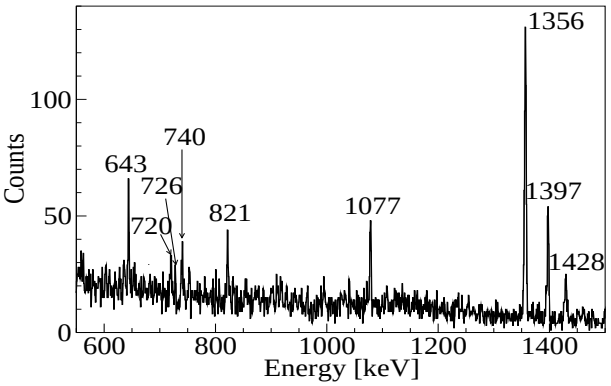

Figure 1: Gamma-ray spectrum obtained for mass A=103+32 in coincidence with positrons. The strongest lines are marked by their energies in keV.

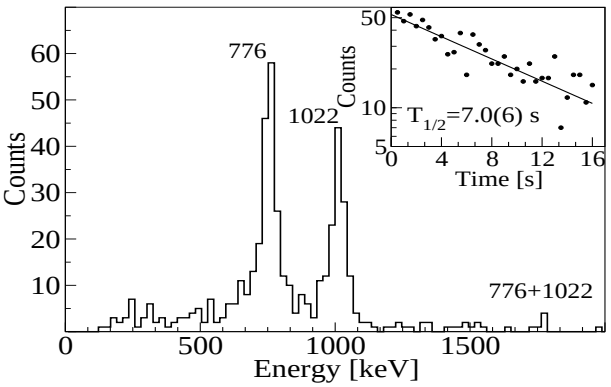

Figure 2: TAS spectrum taken in coincidence with β-delayed protons from the ^{103}Sn decay. The inset shows the time characteristic of β-delayed protons.

References

[1] R. Kirchner, Proc. Conf. to EMIS-14, NIM A, in print
[2] M. Karny *et al.,* contr. GSI Sci. Rep. 2002
[3] I. Mukha *et al.,* contr. GSI Sci. Rep. 2002
[4] J. Szerypo *et al.,* Z. Phys. A 359 (1997) 117
[5] J. Kownacki *et al.,* Nucl. Phys. A627 (1997) 239
[6] P. Tidemand-Petersson *et al.,* Z. Phys. A 302 (1981) 343
[7] K. Rykaczewski, Report GSI-95-09, 1995
[8] A. Stolz, Ph.D. Thesis, TU München (2001)